Stem Cell Reports
Article

OPEN ACCESS

A Non-invasive Platform for Functional Characterization of Stem-Cell-Derived Cardiomyocytes with Applications in Cardiotoxicity Testing

Mahnaz Maddah,[1,*] Julia D. Heidmann,[1] Mohammad A. Mandegar,[2] Chase D. Walker,[1] Sara Bolouki,[1] Bruce R. Conklin,[2,3] and Kevin E. Loewke[1]

[1]Cellogy, Inc., Palo Alto, CA 94301, USA
[2]Gladstone Institute of Cardiovascular Disease, San Francisco, CA 94158, USA
[3]Departments of Medicine, and Cellular and Molecular Pharmacology, University of California, San Francisco, San Francisco, CA 94143, USA
*Correspondence: mmaddah@alum.mit.edu
http://dx.doi.org/10.1016/j.stemcr.2015.02.007

SUMMARY

We present a non-invasive method to characterize the function of pluripotent stem-cell-derived cardiomyocytes based on video microscopy and image analysis. The platform, called Pulse, generates automated measurements of beating frequency, beat duration, amplitude, and beat-to-beat variation based on motion analysis of phase-contrast images captured at a fast frame rate. Using Pulse, we demonstrate recapitulation of drug effects in stem-cell-derived cardiomyocytes without the use of exogenous labels and show that our platform can be used for high-throughput cardiotoxicity drug screening and studying physiologically relevant phenotypes.

INTRODUCTION

Recent advances in stem cell technologies have enabled routine analysis of patient-derived cardiomyocytes, opening up new opportunities for drug testing and personalized health care. Numerous studies have demonstrated that induced pluripotent stem-cell-derived cardiomyocytes (iPS-CMs) display physiologically relevant characteristics and patient-derived iPS-CMs recapitulate aspects of patient cardiac pathology/phenotype in vitro (Harris et al., 2013; Navarrete et al., 2013; Sun et al., 2012). iPS-CMs can be used for preclinical testing of new drugs that may cause drug-induced arrhythmia or QT prolongation and cardiotoxicity, as well as for post-market safety testing or repurposing of existing Food and Drug Administration-approved drugs (Guo et al., 2011; Liang et al., 2013; Sirenko et al., 2013; Himmel, 2013). Improved cell-culturing technologies now allow for the production of well-characterized cardiomyocytes at scale, hence providing a reliable source for routine screening applications. Therefore, accurate and reliable characterization of these cells, and their response to different chemical compounds plays a critical role in their successful utilization in drug development and safety testing.

An ideal platform for characterizing iPS-CMs would ensure reproducibility, require small samples, provide a reliable and comprehensive quantitative profile of cell function, and be cost effective when run at large scales. Label-free video microscopy has already been recognized as a well-suited platform (Makino et al., 1999; Hossain et al., 2010). For example, Ting et al. (2014) created a video-management platform that determines whether a specific region is beating; it segments and counts the beating pattern/signal of differentiated cardiomyocytes with a user-specified threshold on the average change in signal intensity. Also, Ahola et al. (2014) captured the beating activity of single cardiomyocytes by analyzing the motion vector field of individual cells manually segmented by the user. Similarly, researchers estimated beating profiles of cardiomyocytes with a block-matching optical flow approach (Huebsch et al., 2014). While this approach yields vector fields of cellular motion for beating monolayer and single-cell iPSC-CMs, it is computationally expensive and may require manual tuning of the expected motion parameters and signal thresholds for each video. These efforts show the promise of video microscopy and analysis; however, we need an integrated and fully automated solution to characterize iPS-CMs at larger scales. This solution must avoid manually tuning software parameters for each video and also handle a broad range of cell-culture conditions, such as varied cell densities and drug treatments. Finally, to facilitate real-time monitoring at relatively low cost, the algorithms used to identify motion must be rapid and suitable for computational implementation without the need for parallel computing.

In current practice, patch-clamp assays are the standard reference for high-precision electrical measurements of iPS-CMs (Peng et al., 2010). However, patch-clamp analysis requires manual operation by a trained electrophysiologist. Such assays are inherently low-throughput and will not scale to meet the demands of large-scale drug testing. iPS-CMs can also be characterized using electrical potentials captured by a micro-electrode array (MEA) (Harris et al., 2013). With an MEA system, the local potential in a region consisting of electrically active cells is measured as a function of time in order to generate a beating signal that

contains information such as frequency, irregularity, and QT interval. Such systems typically require high cell density in specialized plates and rely on direct contact between cells and electrodes. Other methods, such as fluorescence imaging of the calcium signals (Paredes et al., 2008), can be useful, but are prone to phototoxicity as well as potential interactions between calcium indicators and the chemical compounds being studied (Muschol et al., 1999).

In this paper, we present an all-in-one platform, Pulse, which uses video microscopy and image-analysis algorithms (Maddah and Loewke, 2014) to automatically capture and quantify the beating patterns of cardiomyocytes. Our technique generates a beating signal that corresponds to the biomechanical contraction and relaxation of iPS-CMs, based on motion analysis of phase-contrast images captured at up to 50 frames per second. From the beating signal, various quantitative measurements such as beating frequency, irregularity, and duration of a single contraction are calculated. We designed a set of experiments to validate and test the Pulse platform, performed successfully across 800 different videos, and used a diverse set of compounds to investigate the extent to which Pulse can capture dose-dependent responses of different drugs. Pulse is a fully automated biomechanical contractile analyzer designed to be compatible with common cell-culture practices (using standard multi-well plates) and completely non-invasive to cells, making it ideal for large-scale cardiovascular drug development and cardiotoxicity testing. It is worth mentioning, however, that Pulse is not meant to replace electrophysiology or other methods such as MEA or Ca^{2+} imaging altogether, but to supplement them. We envision applications of Pulse as a primary screening tool that can be used to efficiently and cost-effectively scan large numbers of compounds for cardiotoxicity. Such studies could then be followed up in more detail with fewer and more-targeted patch-clamp assays.

RESULTS

Video Motion Analysis

The Pulse video analysis software extracts and quantifies beating signals from the video of cardiomyocytes. Our method enables automated extraction of quantitative parameters that are of interest in clinical studies from cultures with different cell densities and with either regular or irregular beating patterns. Specifically, it captures and quantifies the biomechanical beating of cardiomyocytes by performing motion analysis on the image sequence to capture changes in the image intensity due to cardiomyocyte contraction and relaxation. The design of our algorithm is guided by the fact that it should be possible to work on different tissue types without the need for any parameter tuning. This is why we avoid the use of specific cell segmentation algorithms and apply a more data-driven approach. Figures 1A–1D diagrams the steps of the Pulse algorithm, which includes (1) block-wise segmentation of the image sequence, (2) extraction of the beating signal for each block, (3) quantification of the beating signals, (4) outlier rejection, and (5) clustering of the beating signals into a set of unique signals, each representing a region of the culture where cardiomyocytes beat in synchrony.

Extraction of Beating Signals

The algorithm first segments each image in the video sequence into 30 non-overlapping blocks. Background blocks, i.e., those that do not contain any cells, are removed from further processing. Then a beating signal is extracted for each block as follows. For every image and each candidate beating block, a one-dimensional vector of pixel intensities is constructed. Starting from the second image in the sequence, the correlation coefficient of intensity vectors of the image and its preceding image in the sequence is computed. Figure 1E shows an example of a beating signal extracted for one of the blocks. This *relative correlation* signal typically exhibits three states: a resting state, where the correlation between successive images is high, a contraction state, and a relaxation state. Although the beating pattern and frequency can be measured from this signal, automatic identification of beating intervals is challenging due to the presence of double peaks and the lack of prior knowledge on their relative magnitude or distances. To obtain a single-peak signal, the algorithm first estimates a reference image by taking the median of resting-state images. An *absolute correlation* signal is then generated by computing the correlation coefficient of the intensity vector of the reference image with those of all images in the sequence. Figure 1F shows an example of the resulting signal.

Quantification of the Beating Signal

To capture irregularity and dynamics of beating profile over time, we perform the analysis in the time domain as opposed to frequency domain. The algorithm first identifies the peaks of the absolute correlation signal. A vector of estimated beating intervals is constructed by calculating the duration between successive peaks. We define the effective beating rate based on the median of the vector and define the irregularity of beating pattern based on the interquartile range (IQR) of the vector. We define the beat duration at 75% (meaning the duration is measured at 25% of the peak magnitude in the absolute correlation signal) and take the average duration over all beats. Finally, peak height, which is a unit-less quantity, is a measure of contractility; stronger contraction results in larger values for the peak height. Figure 1F schematically shows how these measurements are performed on the beating signal.

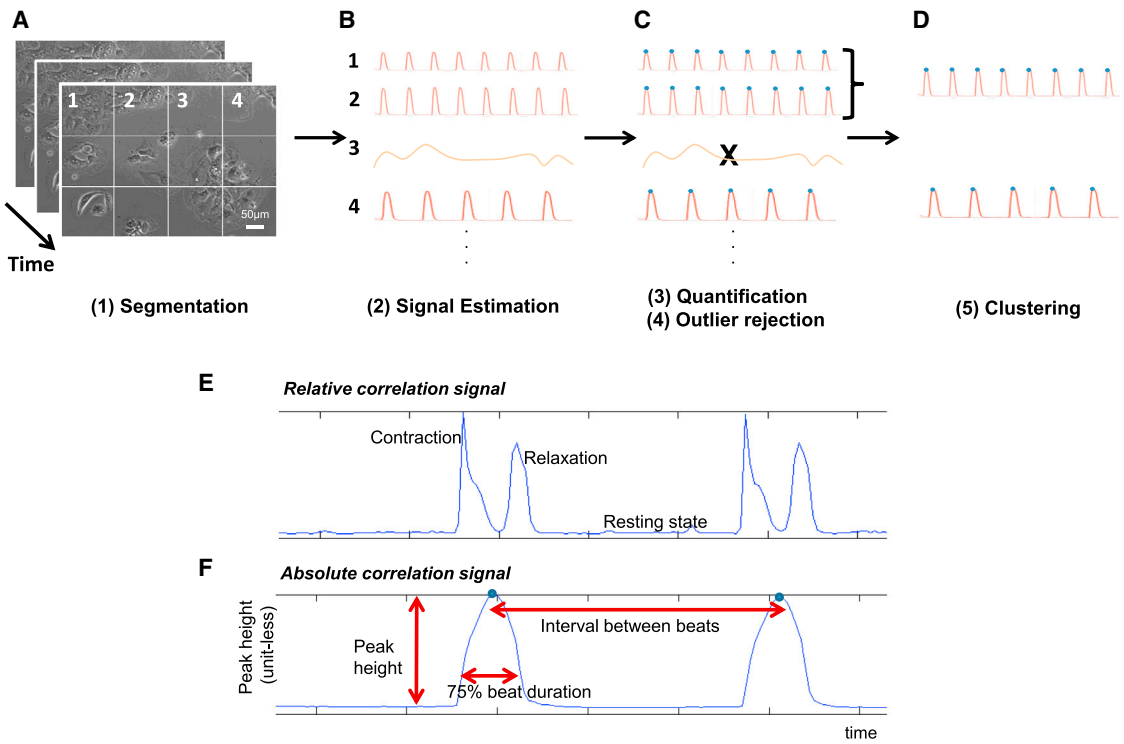

Figure 1. Processing Steps of Pulse Video Analysis

(A) Block-wise segmentation of the image sequence; background blocks are excluded from further processing.

(B) A motion signal is estimated for each block, which can include noisy signals from moving debris.

(C) Signal processing is performed on each signal to identify peaks and model the shape of the beats, and to measure parameters such as frequency and duration. If the beats in a signal are not similar, the signal is identified as outlier and is rejected.

(D) Beating signals with similar pattern are automatically clustered together.

(E) A relative correlation signal is estimated per block.

(F) From the relative correlation signal, the resting state is identified and is used a reference to measure the absolute correlation signal, from which the quantitative parameters are automatically measured.

Outlier Rejection

Once the absolute correlation signal is quantified, we perform outlier rejection. Outliers can consist of noisy signals that occur due to moving debris or bubbles in the media. To keep the arrhythmia signals but reject the outliers, we make the assumption that the beats in a signal should have similar shapes. A Gaussian mixture model is fitted to each beating signal, and the fitting error serves as a metric to detect and reject signals that do not represent beating of cardiomyocytes. Finally, the algorithm merges the valid blocks that have similar beating patterns (Maddah and Loewke, 2014), providing the user with a distinct set of signals per data set. To demonstrate the versatility of the algorithm, Figure 2 shows a set of examples for different plating densities and successful extraction of the beating signal. Figures 2A and 2B are examples of monolayer and tissue-like cultures respectively, where the beating blocks have been identified successfully and clustered together as the cells beat in synchrony. Figure 2C shows an example of single-cell plating density where cells have not formed a syncytium and thus beat asynchronously. In this scenario, the algorithm processes each block, excludes the non-beating blocks, and clusters the blocks with similar beating profile together, assigning a distinct label to each cluster. In this example, there are five beating signals corresponding to the five regions marked in the upper picture of Figure 2C. Clustered regions correspond to regions that do not beat in synchrony.

Comparison of Motion Analysis with Patch Clamp

We designed a series of experiments to validate the Pulse platform and demonstrate its ability to detect and measure drug-induced changes to cardiomyocyte function. In a first experiment, we compared the results of Pulse's motion analysis to data collected by simultaneous manual patch clamp (ChanTest Corporation; see experiment protocol in the Supplemental Experimental Procedures). Phase-contrast imaging and patch-clamp recordings were

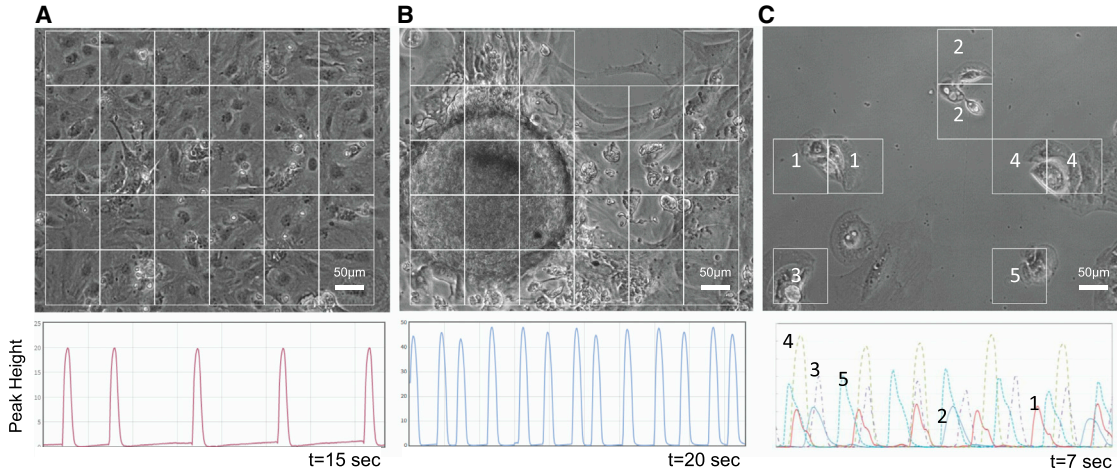

Figure 2. Successful Estimation of Beating Signals on Cardiomyocytes Cultured in Different Conditions

Example of cardiomyocytes with (A) monolayer (cells from Cellular Dynamics), (B) cardio-sphere (cells from Gladstone Institute), (C) single cell (cells from Axiogenesis), corresponding to Movies S1, S2, and S3. In (C), there are five distinct beating signals corresponding to the five regions marked in the upper picture. Clustered regions correspond to regions that do not beat in synchrony.

performed simultaneously on iPSC-derived cardiomyocytes (Cor.4U cell line by Axiogenesis). Figure 3 shows the overlay of the signals measured by these two approaches on three independent cardiomyocyte samples. As observed in the figure, the Pulse beating profiles precisely match the corresponding patch-clamp signals in terms of beating patterns and beat duration. These results confirm that the Pulse system is adequately sampling the beating motion and is generating a reliable output. The manual patch-clamp data were collected while simultaneously capturing a video sequence with a known sampling rate. However, we were not able to record absolute time stamps for both data sets, so the resulting traces were manually aligned.

Comparison of Motion Analysis with Calcium Transients

To compare how calcium transient signals compared to the motion tracings generated by Pulse, we performed two sets of experiments by either modulating calcium transient durations (using quinidine) or inhibiting contraction (using blebbistatin). The biomechanical motion of GCaMP cardiomyocytes (see Figure S1 for a description of genomic modification, cell line derivation, and differentiation) was captured on Pulse, followed by fluorescence video imaging using Keyence BZ-9000 to measure GCaMP fluorescent activity. Video imaging on both microscope systems was repeated after the addition of compound and again after compound washout. Two compounds were used: blebbistatin, which inhibits contraction by blocking myosin II (Abassi et al., 2012), while leaving calcium signaling unaffected, and quinidine, a Na^+ channel blocker, which has been shown to increase action potential duration in human cardiomyocytes (Navarrete et al., 2013; Peng et al., 2010).

Figure 4A shows the beating signal extracted by Pulse 30 min after addition of different concentrations of blebbistatin. As the concentration of blebbistatin is increased, the relative amplitude of the beating signal decreases, serving as a functional readout for the expected reduction in contractility. Figure 4B shows a comparison of the amplitude of the beating signal before blebbistatin is added, 30 min after compound application, and after a subsequent media change. Note that the biomechanical beating of the cardiomyocytes is restored back to normal levels after blebbistatin is washed away. For a concentration of 1 μM or above, no biomechanical beating is observed. In contrast, fluorescence imaging of GCaMP continues to generate a calcium transient signal even at 5 μM, as seen in Figure 5C. These data demonstrate that Pulse is able to capture and quantify the effect of a myosin II blocker in inhibiting the biomechanical contraction of the cardiomyocytes, an effect that MEA or Ca^{+2} imaging systems do not capture (Abassi et al., 2012).

In a second experiment, we applied 3 μM quinidine to GCaMP cardiomyocytes and performed video imaging 30 min after addition of the drug. Using Pulse, we detect a 30% increase in the 75% duration of beat duration and a 40% prolongation of the 75% duration as measured by calcium imaging after drug addition. Figure 4D shows that Pulse and Ca^{2+} imaging detect a comparable increase in the 75% duration, indicating that a prolonged calcium signal correlates with prolonged physical contraction and relaxation.

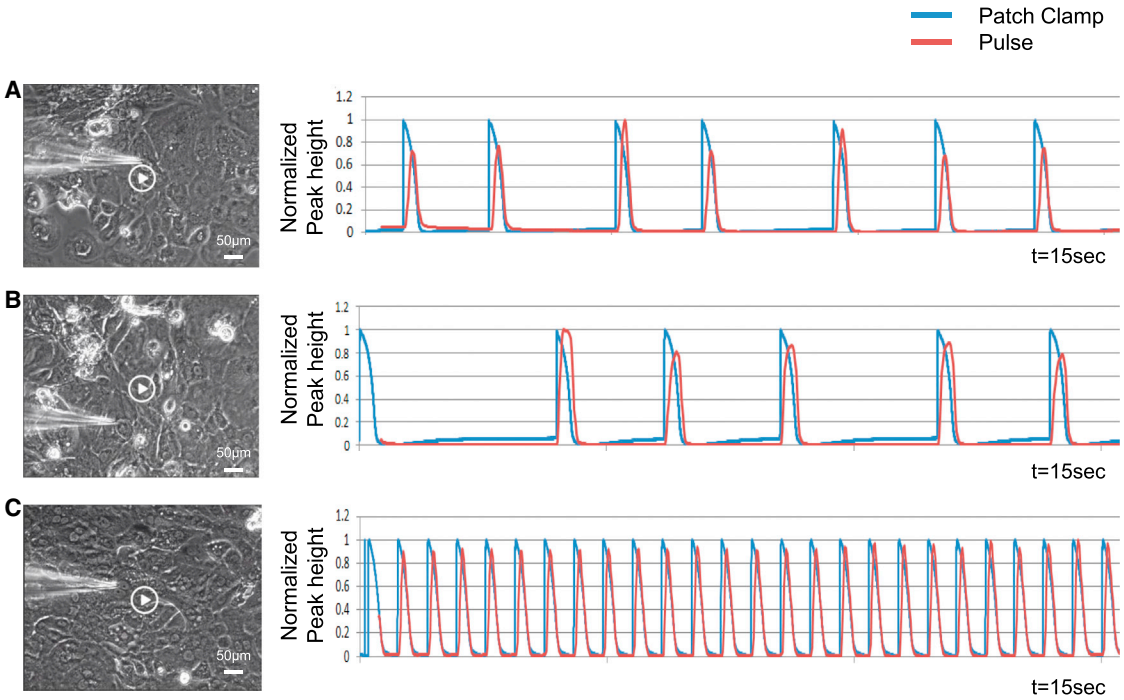

Figure 3. Overlay of Beating Signals Derived from Pulse and Patch Clamp

Patch-clamping data and video were collected concurrently. Motion-analysis-derived and electrophysiologically generated traces for three independent cell cultures (A–C) with varying frequency and irregularity are overlaid, showing similar results.

Pulse Captures Expected Effects of Commonly Used Drugs on iPS-Derived Cardiomyocytes

We performed a set of experiments with a diverse panel of compounds to demonstrate the strength and sensitivity of Pulse in capturing dose-dependent responses to different drugs. In this work, we show the results of eight commonly used drugs with well-known effects on the beating pattern of cardiomyocytes. Table 1 and Figure 5 show a summary of the results. Aspirin was chosen as the negative control, while the other seven drugs have known effects in changing the beat rate, inducing arrhythmias, or changing the action potential duration.

All drugs used for this study were purchased from Sigma-Aldrich, diluted in DMSO, subsequently frozen, and serially diluted in pre-equilibrated media immediately prior to each experiment. Each compound was tested at three concentrations, in replicates of six wells with four recordings from each well. For drug testing experiments, cryo-reserved GCaMP cells were thawed and plated in 24-well plates and allowed 5 days for recovery. Fresh pre-warmed and equilibrated (37°C; 5% CO_2) media were added to the cells 2 hr prior to video imagining on Pulse. To ensure that the compound of interest was homogeneously mixed in the media and to keep the amount of liquid added during each experiment constant, the compound under study was added at a 2× dilution in freshly prepared pre-equilibrated medium and added with a 50% media change on a 37°C plate in a laminar flow hood. This procedure was carried out for all concentrations. To correct for vehicle-dependent effects, control samples underwent media change with the addition of DMSO reflecting the maximum DMSO concentration in test wells. After compound addition, cells were returned to the Pulse system and allowed to equilibrate 30 min prior to imaging to avoid artifacts caused by media addition and temperature change. After the initial sweep, 15 s videos were acquired hourly as described in the Experimental Procedures. A washout step was performed after the experiment; cells were allowed to return to baseline and run on Pulse again after a minimum of 2 hr. Note that Pulse is designed to image the same areas within a plate for each given plate format, so even though plates were removed for media change after baseline measurement, subsequent measurements were taken from the exact same area of the plate.

In each imaging experiment, video microscopy data were collected from four non-overlapping and pre-defined regions in each well of a 24-well plate (resulting in 96 videos per experiment). Each video was subsequently analyzed as described in the Experimental Procedures, generating the measurements of beating frequency, beat-to-beat variation, beat duration, amplitude, and prevalence of beating cells. Videos with beating prevalence of less than 5% were excluded from data analysis. Beat duration was corrected

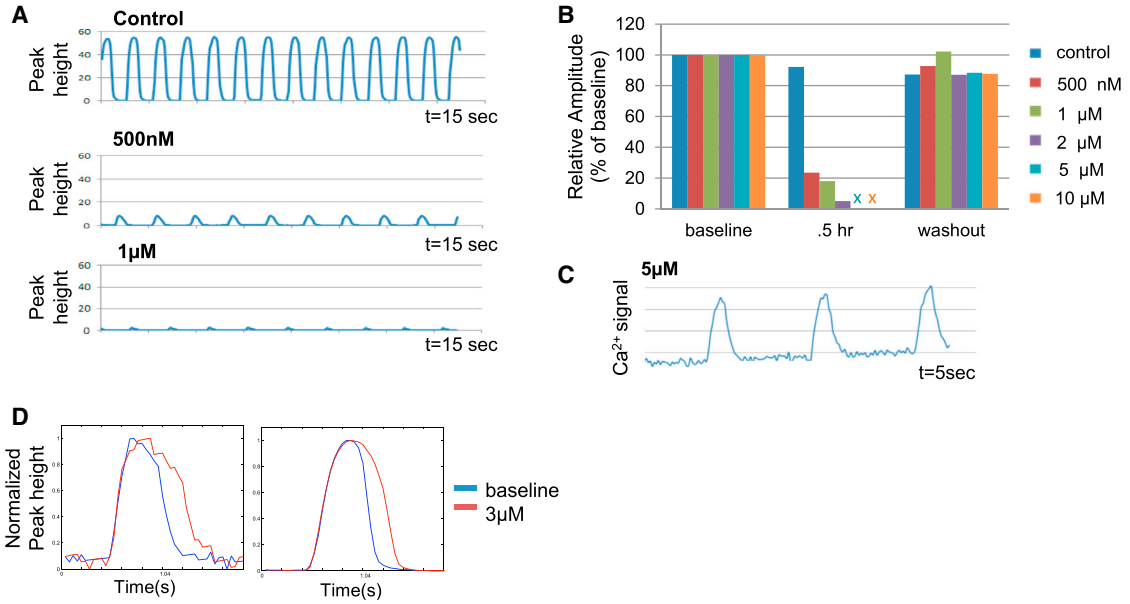

Figure 4. Ca^{2+} Imaging Experiments on GCaMP Cells

(A) Response of the beating signal extracted by Pulse to different doses of blebbistatin. The amplitude of the biomechanical beating signal decreases as the dose increases.

(B) Comparison of the relative amplitude of the biomechanical beating signal before blebbistatin is applied, after 30 min of applying this compound, and after a media change to wash out blebbistatin. Each drug concentration mean value is based on technical replicates of four wells with four recordings per well.

(C) No change is seen in the Ca^{+2} signal.

(D) Beating signal extracted by Pulse and Ca^{2+} imaging with and without quinidine. Both methods capture an increase in the duration of the beats. See also Figure S1 for description of genomic modification of the GCaMP cell line used in these experiments.

using Fridericia's formula (Fridericia, 1920). Figure 5 shows representative examples of beating profiles measured by Pulse and variation induced by drugs. The bar charts on the right show the normalized drug response (e.g., duration) with respect to their baseline, represented by mean and SEM values. The plots in Figure 5 demonstrate that our platform successfully captures and quantifies dose-dependent responses to drugs.

Detection of Changes in Beat Rate

To determine whether Pulse can reliably detect increased or decreased beat rate, we initially tested the effects of two compounds: norepinephrine, a beta adrenergic receptor agonist, and verapamil, which has been shown to act as a negative chronotrope. We observed a dose-dependent increase in beat rate with the addition of norepinephrine (see Figure 5A), while verapamil decreased beat rate at 50 nM (see Figure S2A). Cisapride and E-4031 also decreased the beat rate (see Figures S2B and S2C).

Pulse Detects Prolonged Beat Duration and Arrhythmias upon Inhibiting hERG

The hERG potassium channel is involved in regulating cardiac repolarization. In addition to arrhythmia, drugs that block its function have been associated with long QT syndrome. On an electrophysiological level, this is reflected by increased action potential duration. We reasoned that this should correlate with a change in the duration of physical contraction as measured by Pulse. We tested the effect of various concentrations of hERG inhibitors including cisapride, E-4031, and sotalol and observed an increase in beat duration, as shown in Figures 5B, 5C, and 5F, respectively. This effect was dose dependent, with the exception of cisapride at 200 nM, the respective maximal dose that was used. This may be partially due to cytotoxicity, as we observed beating cessation in several of the 200 nM cisapride-treated samples. Arrhythmias were observed at elevated doses for E-4031 and cisapride, as shown in the traces in Figures 5C and 5B. Notably, this phenomenon was visible in many, but not all, of the samples treated within effected doses, suggesting that the arrhythmia caused by these drugs may be intermittent. We also note that some of the arrhythmias included shorter "twitch"-like beats, which may have impacted the duration measurements. Additional examples are shown in Figure 6, including 96 beating signals estimated by Pulse and successful detection of arrhythmic beats due to addition of cisapride and E-4031.

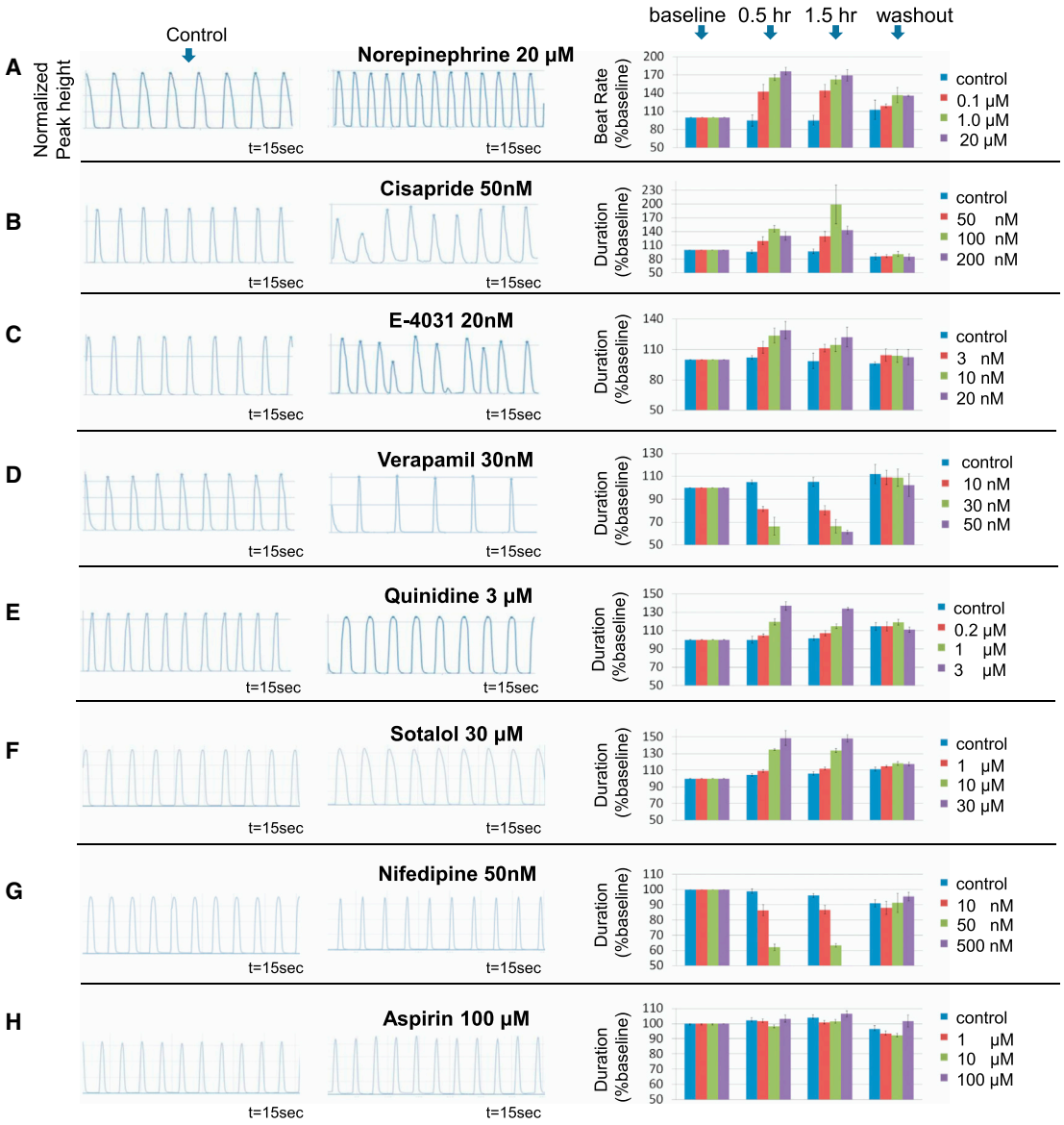

Figure 5. Drug Testing Experiments

We studied and quantified effect of eight drugs by motion analysis of GCaMP cardiomyocytes. The left panel shows the signals estimated from a video of one example region before and after the addition of the drug. The bar charts on the right show the variation of a beating parameter (mean and SEM) for control and different doses at four time points. Each drug concentration included technical replicates of six wells and four recordings per well, for 24 total measurements. The mean values were calculated by first taking the average of within-well replicates, reducing the 24 measurements per concentration from 24 to 6, and then calculating the mean and SEM with n = 6.

(A) Norepinephrine. Our method detects a dose-dependent increase in beat rate and decrease in beat duration.

(B) Cisapride. We detect arrhythmic beating patterns, an increase in beat duration, and decrease in beat rate.

(C) E-4031. We detect an arrhythmic beating patterns, an increase in beat duration, and decrease in beat rate.

(D) Verapamil. Our method detects significant decrease in beat duration, as well as decrease in beat rate at high concentrations.

(E) Quinidine. Our method detects a dose-dependent increase in beat duration and decrease in beat rate.

(F) Sotalol. Our method detects a dose-dependent increase in the beat duration.

(G) Nifedipine. Our method detects a dose-dependent increase in the beat duration.

(H) Aspirin. We detect no significant change in beat rate, irregularity, or duration.

See also Figure S2.

Table 1. Screening the Effect of Drugs on iPSC-Derived Cardiomyocytes

Drug Name	Mode of Action	Expected Effect	Pulse Readout
Norepinephrine	B-AR agonist	increased beat rate (Peng et al., 2010, at 0.1 μM)	increased beat rate (0.1, 1, and 20 μM)
Cisapride	hERG inhibitor	arrhythmia, duration prolongation (Liang et al. [2013] at 30 nM; Harris et al. [2013] at 3 nM, statistically significant at 100 nM)	arrhythmia, duration prolongation (50, 100, and 200 nM)
Quinidine	Na^+/L-type Ca^{2+} channel blocker, hERG inhibitor	duration prolongation (Peng et al. [2010] at 0.1 μM; Harris et al. [2013] at 0.3 μM)	duration prolongation (0.2, 1, and 3 μM)
Verapamil	L-type Ca^{2+} channel blocker, hERG inhibitor	Duration shortening (Harris et al., 2013, at 30 nM)	duration shortening (10, 30, and 50 nM)
E-4031	hERG inhibitor	arrhythmia, duration prolongation (Peng et al. [2010] at 3 nM; Harris et al. [2013] at 3 nM)	arrhythmia, duration prolongation (3 and 10 nM)
Sotalol	B-AR/hERG inhibitor	duration prolongation (Peng et al. [2010] at 3 μM)	duration prolongation (10 and 30 μM)
Nifedipine	L-type Ca^{2+} channel blocker	duration shortening (Peng et al. [2010] at 30 nM; Harris et al. [2013] at 30 nM)	duration shortening (10 and 50 nM)
Aspirin	NSAID	none	none

Expected effects are from published literature. See also Table S1.

Multi-effect Compounds

Having shown that Pulse is able to detect increases in beat duration associated with hERG channel inhibition, we performed additional verification experiments with inhibitors of other ion channels, including quinidine, verapamil, and nifedipine. Quinidine is a class I antiarrhythmic. Primarily a sodium channel blocker, it also affects calcium and potassium current. As expected, addition of quinidine increased beat duration at all concentrations tested (Figure 5E). In contrast, verapamil and nifedipine, L-type calcium channel blockers, both caused a robust dose-dependent decrease in the beat duration (Figures 5D and 5G). We also observed a decrease in the peak height (motion amplitude) with a nifedipine dose of 50 nM, although not statistically significant, while at the 500 nM the motion signal is completely inhibited (Figure S2D). Additionally, aspirin, a non-steroidal anti-inflammatory drug (NSAID), which should have no effect on cardiomyocyte activity, was run as a negative control and shown not to alter any of the parameters measured by Pulse (Figure 5H). Table 1 summarizes the results of drug screening studies performed in this study, which show similar trends to the expected effects from published literature. Table S1 reports values for the motion signal measured by Pulse and APD_{90} values reported in Peng et al. (2010) for a subset of data with comparable drug concentrations. While differences in cell lines and protocols prevent a direct comparison, Table S1 confirms that similar trends are seen between motion data and action potential data.

DISCUSSION

In this paper, we presented Pulse as an integrated video microscopy and image-analysis software platform that enables impartial and unbiased biomechanical motion analysis of cardiomyocytes in a high-throughput manner. The platform enables users to use standard tissue culture format vessels to analyze the contractile properties of in-vitro-derived human cardiomyocytes without detailed knowledge of electrophysiology. Moreover, Pulse is robust enough that it is capable of analyzing single cells seeded at low density, in a monolayer or in 3D culture format without additional input or parameter modification from the user. Pulse is also completely automated, making it easy to use and amenable to high-throughput studies, without the need for extensive post acquisition data processing.

While methods such as manual patch clamp provide detailed information of the electrical activity of cardiomyocytes, these methods are time consuming and require the expertise of a trained electrophysiologist. In addition, these methods are invasive, and generally a single recording can be performed on the cells at a single time point, hence making it difficult to perform longitudinal and long-term studies on the same set of cells.

Using Pulse, we have demonstrated recapitulation of well-characterized drug effects in iPSC-derived cardiomyocytes. This platform can be used for high-throughput cardiotoxicity drug screens and studying physiologically relevant disease phenotypes such as arrhythmias observed

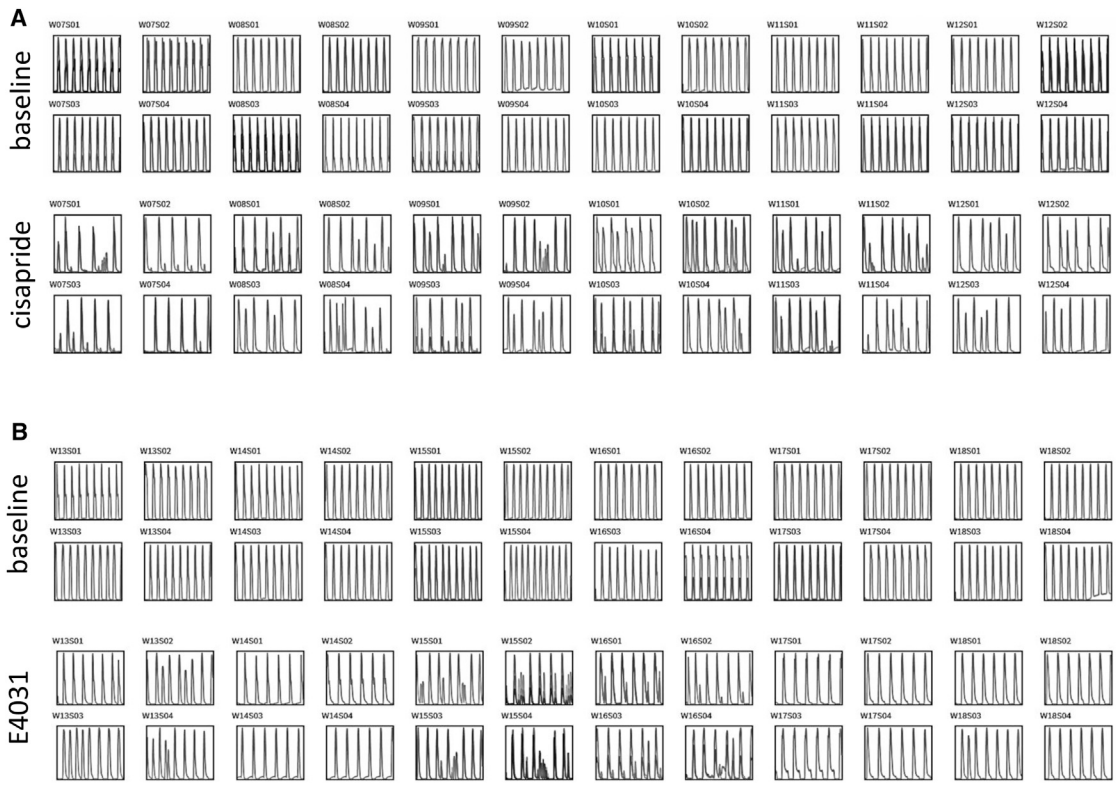

Figure 6. Extracted Beating Signals by Pulse

The plots demonstrate successful detection of arrhythmic beats due to addition of (A) cisapride (50 nm) and (B) E-4031 (10 nm) to the iPS-CMs from Cellular Dynamics. (A) and (B) are two independent experiments. In each experiment, signals from a single row of a 24-well plate are shown for four samples per well (total of 24) before and after the addition of drug. Signals are recorded over the duration of 15 s with 24 images per second.

in long QT syndrome (Spencer et al., 2014), and abnormal calcium handling and contractile properties in hypertrophic and dilated cardiomyopathy disease models (Lan et al., 2013; Sun et al., 2012). In addition, the high-throughput capabilities of Pulse enable the detection of subtle cellular phenotypes that may otherwise be undetectable due to cell-to-cell variability of the differentiated iPS-CM.

One current limitation of the Pulse system is the time lag between one video capture to the next. For example, using a 96-well format, there is 25-min time lag from the first video acquisition to the 96th well seconds of recording at 15-s video recordings. This serial scanning time lag limits the use of Pulse for high-throughput analysis of fast drug responses. To address this issue, a lower throughput vessel format (e.g., 6-well plate) can be used. Future development of the Pulse platform will include a microfluidic drug delivery system to enable high-throughput analysis of fast drug responses.

Additional future development of the platform will include the addition of a fluorescence imaging module to allow simultaneous and multi-modal analysis of cardiomyocytes in a single platform, as well as a mechanism to pace the cells electrically.

EXPERIMENTAL PROCEDURES

Video Microscopy

The Pulse imaging system includes a digital inverted phase-contrast microscope with a 10× phase objective lens, 625-nm LED for illumination, and high-speed CMOS camera for image capturing. The microscope platform is integrated with a high-precision motorized xy stage, which enables scanning of standard multi-well plates (6- to 96-well), and a high-quality stage-top incubator that keeps the temperature and CO_2 levels uniform. Images are captured by the camera at a rate of 24 frames/s at 640 × 480 resolution, which is adequate for sampling the beating pattern of iPS-CMs. Prior to acquisition of each run, the system resets the stage and then moves the stage automatically and sequentially to image one or more locations per well, performs auto-focus to find the optimal focal plane, and subsequently captures a high-frame-rate image sequence for the duration specified by the user (typically 10–20 s).

iPSC-Derived Cardiomyocytes

To evaluate the performance of Pulse in various cell-culture conditions and experimental settings, we performed series of experiments using human iPSC-derived cardiomyocytes from three independent sources including two commercially available cells (Axiogenesis and Cellular Dynamics) as well as a genetically engineered calcium indicator line (GCaMP). Cryo-preserved cardiomyocytes were thawed and plated in different multi-well plate formats (6- to 96-well) and seeded at various densities to obtain single cells, small cell clusters, and monolayers.

Axiogenesis and Cellular Dynamics iPS-CMs

Cryo-preserved cardiomyocytes were thawed, plated, and maintained according to manufacturer's instructions on matrigel with manufacturer supplied (proprietary) media. Cells were plated at different densities: axiogenesis cardiomyocytes were plated at 10,000–20,000/well in 96-well format and at 43,000–125,000 in 24-well format. Cellular Dynamics cardiomyocytes were plated at densities between 50,000 and 150,000/well in 24-well format. Cells were allowed to recover for a minimum of 10 days after thawing before experimental use. This was dependent on the time it took for beating parameters to stabilize and reach cell-line-specific expected values.

GCaMP6f iPSC-Derived Cardiomyocytes

To enable high-throughput and non-invasive monitoring of Ca^{2+} transients of cardiomyoyctes, the GCaMP iPSCs were generated using transcription activator like effector nuclease (TALEN)-mediated targeting of the GCaMP6f (Chen et al., 2013) open reading frame into the AAVS1 safe harbor locus (Hockemeyer et al., 2011). The GCaMP6f ORF is driven off a strong constitutive promoter (CAG), which remains transcriptionally active in the AAVS1 locus in different cell types and iPS-derived cardiomyocytes, enabling monitoring of high signal-to-noise ratio.

The GCaMP iPSC lines were differentiated into iPS-CM using the Wnt modulation differentiation method (Lian et al., 2012). In brief, iPSCs were treated with 12 μM CHIR99021 (CHIR) in RPMI/B27 without insulin for 24 hr on day 0, and 5 μM IWP2/RPMI/B27 without insulin was added on day 3. On day 7, the media was switched to RPMI/B27 with insulin. On day 15, the cells were dissociated into single cells using EDTA and cryo-preserved in FBS+10% DMSO. For experiments, induced cardiomyocytes were plated at various densities (5,000–42,000/well in 96-well format and 50,000–110,000/well in 24-well format) on matrigel in RPMI/B27 with insulin.

SUPPLEMENTAL INFORMATION

Supplemental Information includes Supplemental Experimental Procedures, two figures, one table, and three movies and can be found with this article online at http://dx.doi.org/10.1016/j.stemcr.2015.02.007.

ACKNOWLEDGMENTS

The authors would like to thank Nathaniel Huebsch for his constructive input. This work was funded in part by the NIH grant R44 HL126277-01. M.M. and K.L. are employees and shareholders in Cellogy, Inc.

Received: October 23, 2014
Revised: February 11, 2015
Accepted: February 11, 2015
Published: March 19, 2015

REFERENCES

Abassi, Y.A., Xi, B., Li, N., Ouyang, W., Seiler, A., Watzele, M., Kettenhofen, R., Bohlen, H., Ehlich, A., Kolossov, E., et al. (2012). Dynamic monitoring of beating periodicity of stem cell-derived cardiomyocytes as a predictive tool for preclinical safety assessment. Br. J. Pharmacol. *165*, 1424–1441.

Ahola, A., Kiviaho, A.L., Larsson, K., Honkanen, M., Aalto-Setälä, K., and Hyttinen, J. (2014). Video image-based analysis of single human induced pluripotent stem cell derived cardiomyocyte beating dynamics using digital image correlation. Biomed. Eng. Online *13*, 39.

Chen, T.-W., Wardill, T.J., Sun, Y., Pulver, S.R., Renninger, S.L., Baohan, A., Schreiter, E.R., Kerr, R.A., Orger, M.B., Jayaraman, V., et al. (2013). Ultrasensitive fluorescent proteins for imaging neuronal activity. Nature *499*, 295–300.

Fridericia, L.S. (1920). The duration of systole in the electrocardiogram of normal subjects and of patients with heart disease. Acta Med. Scand. (53), 469–486.

Guo, L., Abrams, R.M., Babiarz, J.E., Cohen, J.D., Kameoka, S., Sanders, M.J., Chiao, E., and Kolaja, K.L. (2011). Estimating the risk of drug-induced proarrhythmia using human induced pluripotent stem cell-derived cardiomyocytes. Toxicol. Sci. *123*, 281–289.

Harris, K., Aylott, M., Cui, Y., Louttit, J.B., McMahon, N.C., and Sridhar, A. (2013). Comparison of electrophysiological data from human-induced pluripotent stem cell-derived cardiomyocytes to functional preclinical safety assays. Toxicol. Sci. *134*, 412–426.

Himmel, H.M. (2013). Drug-induced functional cardiotoxicity screening in stem cell-derived human and mouse cardiomyocytes: effects of reference compounds. J. Pharmacol. Toxicol. Methods *68*, 97–111.

Hockemeyer, D., Wang, H., Kiani, S., Lai, C.S., Gao, Q., Cassady, J.P., Cost, G.J., Zhang, L., Santiago, Y., Miller, J.C., et al. (2011). Genetic engineering of human pluripotent cells using TALE nucleases. Nat. Biotechnol. *29*, 731–734.

Hossain, M.M., Shimizu, E., Saito, M., Rao, S.R., Yamaguchi, Y., and Tamiya, E. (2010). Non-invasive characterization of mouse embryonic stem cell derived cardiomyocytes based on the intensity variation in digital beating video. Analyst (Lond.) *135*, 1624–1630.

Huebsch, N., Loskill, P., Mandegar, M.A., Marks, N.C., Sheehan, A.S., Ma, Z., Mathur, A.A., Nguyen, T.N., Yoo, J.C., Judge, L.M., et al. (2014). Automated video-based analysis of contractility and calcium flux in human iPS-derived cardiomyocytes cultured over different spatial scales. Tissue Eng. Part C Methods. Published online October 14, 2014. http://dx.doi.org/10.1089/ten.tec.2014.0283.

Lan, F., Lee, A.S., Liang, P., Sanchez-Freire, V., Nguyen, P.K., Wang, L., Han, L., Yen, M., Wang, Y., Sun, N., et al. (2013). Abnormal calcium handling properties underlie familial hypertrophic cardiomyopathy pathology in patient-specific induced pluripotent stem cells. Cell Stem Cell *12*, 101–113.

Lian, X., Hsiao, C., Wilson, G., Zhu, K., Hazeltine, L.B., Azarin, S.M., Raval, K.K., Zhang, J., Kamp, T.J., and Palecek, S.P. (2012). Robust cardiomyocyte differentiation from human pluripotent stem cells via temporal modulation of canonical Wnt signaling. Proc. Natl. Acad. Sci. USA *109*, E1848–E1857.

Liang, P., Lan, F., Lee, A.S., Gong, T., Sanchez-Freire, V., Wang, Y., Diecke, S., Sallam, K., Knowles, J.W., Wang, P.J., et al. (2013). Drug screening using a library of human induced pluripotent stem cell-derived cardiomyocytes reveals disease-specific patterns of cardiotoxicity. Circulation *127*, 1677–1691.

Maddah, M., and Loewke, K. (2014). Automated, Non-invasive Characterization of Stem Cell-Derived Cardiomyocytes from Phase-Contrast Microscopy, Medical Image Computing and Computer-Assisted Intervention (Boston: MICCAI).

Makino, S., Fukuda, K., Miyoshi, S., Konishi, F., Kodama, H., Pan, J., Sano, M., Takahashi, T., Hori, S., Abe, H., et al. (1999). Cardiomyocytes can be generated from marrow stromal cells in vitro. J. Clin. Invest. *103*, 697–705.

Muschol, M., Dasgupta, B.R., and Salzberg, B.M. (1999). Caffeine interaction with fluorescent calcium indicator dyes. Biophys. J. *77*, 577–586.

Navarrete, E.G., Liang, P., Lan, F., Sanchez-Freire, V., Simmons, C., Gong, T., Sharma, A., Burridge, P.W., Patlolla, B., Lee, A.S., et al. (2013). Screening drug-induced arrhythmia [corrected] using human induced pluripotent stem cell-derived cardiomyocytes and low-impedance microelectrode arrays. Circulation *128* (11, Suppl 1), S3–S13.

Paredes, R.M., Etzler, J.C., Watts, L.T., Zheng, W., and Lechleiter, J.D. (2008). Chemical calcium indicators. Methods *46*, 143–151.

Peng, S., Lacerda, A.E., Kirsch, G.E., Brown, A.M., and Bruening-Wright, A. (2010). The action potential and comparative pharmacology of stem cell-derived human cardiomyocytes. J. Pharmacol. Toxicol. Methods *61*, 277–286.

Sirenko, O., Crittenden, C., Callamaras, N., Hesley, J., Chen, Y.-W., Funes, C., Rusyn, I., Anson, B., and Cromwell, E.F. (2013). Multiparameter in vitro assessment of compound effects on cardiomyocyte physiology using iPSC cells. J. Biomol. Screen. *18*, 39–53.

Spencer, C.I., Baba, S., Nakamura, K., Hua, E.A., Sears, M.A.F., Fu, C.C., Zhang, J., Balijepalli, S., Tomoda, K., Hayashi, Y., et al. (2014). Calcium transients closely reflect prolonged action potentials in iPSC models of inherited cardiac arrhythmia. Stem Cell Reports *3*, 269–281.

Sun, N., Yazawa, M., Liu, J., Han, L., Sanchez-Freire, V., Abilez, O.J., Navarrete, E.G., Hu, S., Wang, L., Lee, A., et al. (2012). Patient-specific induced pluripotent stem cells as a model for familial dilated cardiomyopathy. Sci. Transl. Med. *4*, 30ra47.

Ting, S., Liew, S.J., Japson, F., Shang, F., Chong, W.K., Reuveny, S., Tham, J.Y., Li, X., and Oh, S. (2014). Time-resolved video analysis and management system for monitoring cardiomyocyte differentiation processes and toxicology assays. Biotechnol. J. *9*, 675–683.